Quantum State Transfer over 1200 km Assisted by Prior Distributed Entanglement

Bo Li,[1,2,3,*] Yuan Cao,[1,2,3,*] Yu-Huai Li,[1,2,3] Wen-Qi Cai,[1,2,3] Wei-Yue Liu,[1,2,3] Ji-Gang Ren,[1,2,3] Sheng-Kai Liao,[1,2,3] Hui-Nan Wu,[1,2,3] Shuang-Lin Li,[1,2,3] Li Li,[1,2,3] Nai-Le Liu,[1,2,3] Chao-Yang Lu,[1,2,3] Juan Yin,[1,2,3] Yu-Ao Chen,[1,2,3] Cheng-Zhi Peng,[1,2,3] and Jian-Wei Pan[1,2,3]

[1]*Hefei National Laboratory for Physical Sciences at the Microscale and Department of Modern Physics, University of Science and Technology of China, Hefei 230026, China*

[2]*Shanghai Branch, CAS Center for Excellence in Quantum Information and Quantum Physics, University of Science and Technology of China, Shanghai 201315, China*

[3]*Shanghai Research Center for Quantum Sciences, Shanghai 201315, China*

(Received 18 April 2021; accepted 16 March 2022; published 26 April 2022)

Long-distance quantum state transfer (QST), which can be achieved with the help of quantum teleportation, is a core element of important quantum protocols. A typical situation for QST based on teleportation is one in which two remote communication partners (Alice and Bob) are far from the entanglement source (Charlie). Because of the atmospheric turbulence, it is challenging to implement the Bell-state measurement after photons propagate in atmospheric channels. In previous long-distance free-space experiments, Alice and Charlie always perform local Bell-state measurement before the entanglement distribution process is completed. Here, by developing a highly stable interferometer to project the photon into a hybrid path-polarization dimension and utilizing the satellite-borne entangled photon source, we demonstrate proof-of-principle QST at the distance of over 1200 km assisted by prior quantum entanglement shared between two distant ground stations with the satellite *Micius*. The average fidelity of transferred six distinct quantum states is 0.82 ± 0.01, exceeding the classical limit of $2/3$ on a single copy of a qubit.

DOI: 10.1103/PhysRevLett.128.170501

Transferring a quantum state over arbitrary distances based on quantum teleportation [1] allows an unknown quantum state to be measured by Bell-state measurement (BSM) at one location and subsequently reconstructed at another remote location. It can be applied in many important quantum information protocols [2–6]. Thus far, it has been achieved with various technologies, such as photonic qubits [7–12], nuclear magnetic resonance [13], optical modes [14,15], atomic ensembles [16], trapped atoms [17,18], and solid-state systems [19,20]. The first experimental demonstration was reported by the Innsbruck [7] and Rome groups [8] in 1997. Compared with the initial proposal by Bennett and colleagues [1], the Rome scheme is limited in that an unknown quantum state cannot directly come from the outside [21]. Even so, the Rome scheme is generally regarded as the two-photon version implementation of quantum teleportation with the advantage of allowing a full single-photon Bell-state measurement [2].

In quantum teleportation, BSM enables the quantum part of information transferred across a distance. As a result, a unique feature of teleportation is the unlimited distance in theory, which is critical for large-scale quantum communication. Up to now, the longest distance achieved on Earth's surface has been limited to approximately 100 km, in both the optical fiber [22–26] and the terrestrial free-space channel [9–11]. To overcome high loss in the terrestrial channel and Earth's curvature, a promising method involves utilizing a satellite, as the equivalent thickness of the vertical atmosphere is only 5–10 km [27]. We have developed a satellite called "*Micius*" dedicated to quantum science experiments. It was successfully launched on 16 August, 2016, from China and orbits at approximately 500 km. Recently, a series of quantum science experiments have been conducted in space based on this satellite [12,28–35], including ground-to-satellite quantum teleportation [12], which takes the first step toward realizing global-scale quantum communication.

Despite many achievements in previous experiments, they were usually accomplished without a prior entanglement distribution over long distances [9–12]. *Micius* has demonstrated the possibility of distributing entanglement to two ground stations over a thousand kilometers [30], providing a scientific platform for quantum communication applications [29,34]. In this study, by following the Rome scheme and using the prior distributed entangled photons, we implement quantum state transfer (QST) between two ground stations 1200 km apart. The demonstration of QST is proof of principle at present, and it requires the combination of practical quantum memory and feed-forward procedure for complete implementation in the future. The development of an all-optical bonding and high-stable interferometer improved the compatibility with photon source, making it possible for photon stable interference after long-distance transmission in free-space channels [36,37].

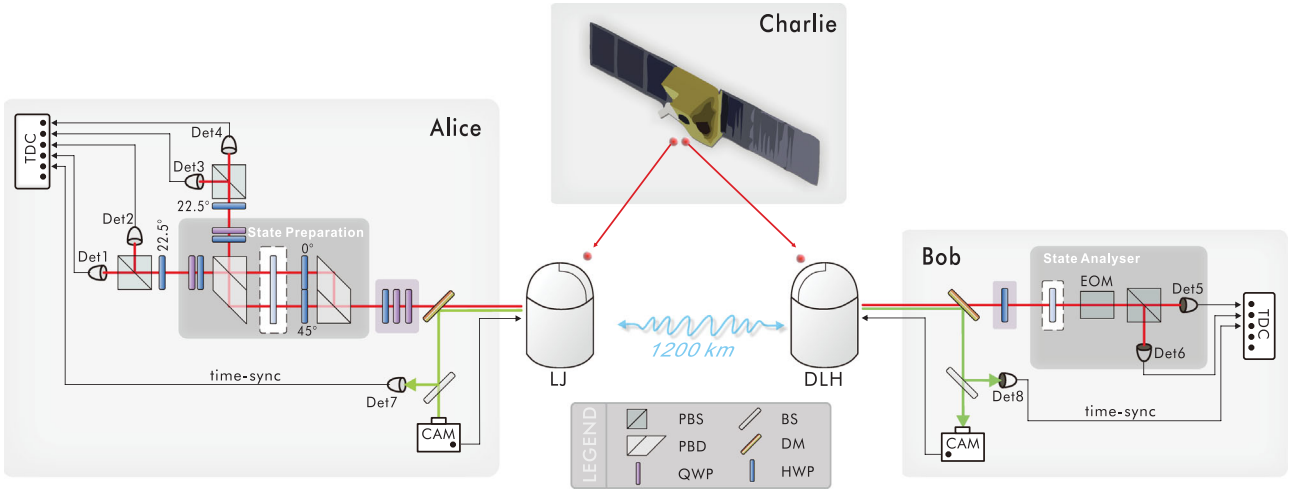

FIG. 1. 1200 km QST assisted by satellite-based entanglement distribution. The *Micius* satellite carried an entangled photon source in the low-Earth orbit. The separation between the DLH and LJ ground stations was approximately 1200 km. Through each pass of the satellite, *Micius* distributed the entangled photon pairs to the telescope in the ground station through the downlink optical channel. The green laser from the satellite functioned as not only the beacon for tracking in the camera, but also the pulse for time synchronization. At the LJ station, after being collected by the telescope, photons passed through a combination of three wave plates for polarization compensation. As state preparation, the MZI divided the photon into two paths based on the polarization. The initial state was prepared by inserting wave plates in the dashed area inside the MZI. After passing through the MZI, the photons were divided into four detectors by 22.5° HWP and PBS, functioning as the Bell-state analysis configuration. At Bob's site, because the telescope was polarization maintained, only one HWP was used to rotate the polarization direction. A wave plate, the EOM, and the PBS worked as the state analyzer to project the photon into an orthogonal basis. All photon detection events and the time-synchronization signal were recorded into the TDC for analysis off-line. Det1–Det 8, single-photon detectors; PBS, polarizing beam splitter; PBD, polarizing beam displacer; DM, dichroic mirror; QWP, quarter-wave plate; HWP, half-wave plate; EOM, electro-optical modulator.

A schematic figure of our experiment is provided in Fig. 1. This experiment involves three parties: Alice, Bob, and Charlie. Alice and Bob are two communication parties of QST. Alice is located at the Lijiang (LJ) observatory of China (26°41'38.15"N, 100°1'45.55"E) to prepare the initial state, and Bob is located at the Delingha (DLH) observatory of China (37°22'44.43"N, 97°43'37.01"E) to validate the final state. The physical distance between Alice and Bob is 1203 km. At Charlie's site, the *Micius* satellite carries a sophisticated compact source of entangled photon pairs. The entangled photon state is close to one of four maximally entangled two-qubit Bell states:

$$|\Psi\rangle_{12} = \frac{1}{\sqrt{2}}(|H\rangle_1|V\rangle_2 + |V\rangle_1|H\rangle_2), \tag{1}$$

where H and V denote horizontal and vertical polarization, respectively, and the subscripts 1 and 2 label the photons in the entangled pair. The brightness of the entanglement source is approximately 5.9 million pairs per second with a pump power of ~30 mW [30]. The source fidelity can be tested by sampling 1% of each path of the entangled photon pairs for on-satellite analysis and optimized remotely. In this Letter, the average state fidelity was tested as 0.927 ± 0.003 on the H/V and $+/-$ basis.

The satellite is equipped with two independent transmission telescopes with apertures of 300 and 180 mm to establish two satellite-to-ground downlink optical channels. Through satellite-borne telescopes, each photon of the entangled pairs individually propagates down toward two ground stations. The ground stations possess receiving telescopes with diameters of 1800 (LJ) and 1200 mm (DLH). Both transmitters on the satellite and receivers on the ground employ the cascaded multistage high-precision closed-loop acquiring, pointing, and tracking (APT) technology. The closed-loop feedback control has a measured accuracy of 0.41 μrad. In each passing of the *Micius* satellite, when the satellite reaches a 5° elevation angle, the beacon lasers on the ground (532 nm) and the satellite (671 nm) point to each other, and the APT system works to establish a downlink channel. When the satellite reaches a 10° elevation angle, the entanglement source begins to generate photon pairs and transfer them down through the channels. Photon 1 is transmitted to the LJ observatory, while photon 2 is transmitted to the DLH observatory.

At Alice's site (LJ ground station), the telescope is not polarization maintained, which will introduce a phase related to the pointing direction. A combination of two quarter-wave plates (QWPs) and one half-wave plate (HWP) was employed to compensate the phase and align the polarization axis in real time. The typical standard deviation of measured wave-plates' angle is less than 1°. The full BSM is performed using a Mach-Zehnder interferometer (MZI) to project the received photons from

polarization into hybrid polarization path dimensions. In the MZI, photon 1 was divided into two parallel path modes according to the polarization on a polarizing beam displacer (PBD). The transmitted or reflected path in H/V polarization is written as $|H\rangle_1 \Rightarrow |H\rangle_1|T\rangle_1$, $|V\rangle_1 \Rightarrow |V\rangle_1|R\rangle_1$, where T and R denote transmission and reflection path mode, respectively. A 45° HWP was inserted in the transmission path to rotate the polarization into $|H\rangle_1|T\rangle_1 \Rightarrow |V\rangle_1|T\rangle_1$. An equally thick 0° HWP is inserted in the reflected path for path compensation. The polarization mode on two paths was indistinguishable. On the second PBD in MZI, the photon was well interfered, and the phase was fixed to zero with HWP and QWP. The polarization-entangled state was transformed into a hybrid path-polarization state, as $|V\rangle_1 \otimes (1/\sqrt{2})(|T\rangle_1|V\rangle_2 + |R\rangle_1|H\rangle_2)$. A combination of HWP and QWP can be inserted inside MZI [vacant area of the MZI in Fig. 1(a)] to rotate the polarization on both paths simultaneously into the initial state to be transferred $|\chi\rangle_1 = \alpha|H\rangle_1 + \beta|V\rangle_1$ with $|\alpha|^2 + |\beta|^2 = 1$. We define four Bell states in the hybrid path-polarization dimension as $|\Psi^{\pm}\rangle_1 = |T\rangle_1|V\rangle_1 \pm |R\rangle_1|H\rangle_1$, $|\Phi^{\pm}\rangle_1 = |T\rangle_1|H\rangle_1 \pm |R\rangle_1|V\rangle_1$. The hybrid state can be rewritten as

$$
\begin{aligned}
|\Psi'\rangle_{12} &= (\alpha|H\rangle_1 + \beta|V\rangle_1) \otimes \frac{1}{\sqrt{2}}(|T\rangle_1|V\rangle_2 + |R\rangle_1|H\rangle_2) \\
&= \frac{1}{2}(|\Psi^-\rangle_1 + |\Phi^-\rangle_1\hat{\sigma}_x - |\Phi^+\rangle_1 i\hat{\sigma}_y - |\Psi^+\rangle_1\hat{\sigma}_z) \\
&\quad (\alpha|H\rangle_2 + \beta|V\rangle_2), \qquad (2)
\end{aligned}
$$

where $\hat{\sigma}_x$, $\hat{\sigma}_y$, and $\hat{\sigma}_z$ denote Pauli operators.

The Bell states $|\Psi^{\pm}\rangle_1$ and $|\Phi^{\pm}\rangle_1$ exits two different ports of the MZI. We arrange the polarization analysis along the $\pm 45°(+/-)$ basis with a 22.5° HWP and a polarization beam splitter (PBS) to discriminate $|\Psi^+\rangle_1/|\Psi^-\rangle_1$ and $|\Phi^+\rangle_1/|\Phi^-\rangle_1$. Four output modes were measured by four single-photon detectors, with each detector's clicks corresponding to one of four Bell states so that all four Bell states could be fully distinguished. The joint BSM on photon 1 at Alice's site could probabilistically make Bob's photon 2 collapse into one of four corresponding states.

To implement successful QST, an interferometer with high visibility (or fidelity) is crucial to implement BSM. In practice, the entangled photons received at the ground stations propagate thousands of kilometers down from the satellite. Therefore, before the photon enters the MZI, its optical wavefront is distorted by the atmospheric turbulence, which results in a multimode field. We make a rough numerical estimate, achieving a high visibility such as 96%; the tolerance of the optical component's misalignment in the MZI is about 20 μm of transverse position and 13 μrad of angular tilt. Moreover, our MZI is mounted in LJ where the outdoor environment varies, and the long-term stability of the phase is difficult to achieve.

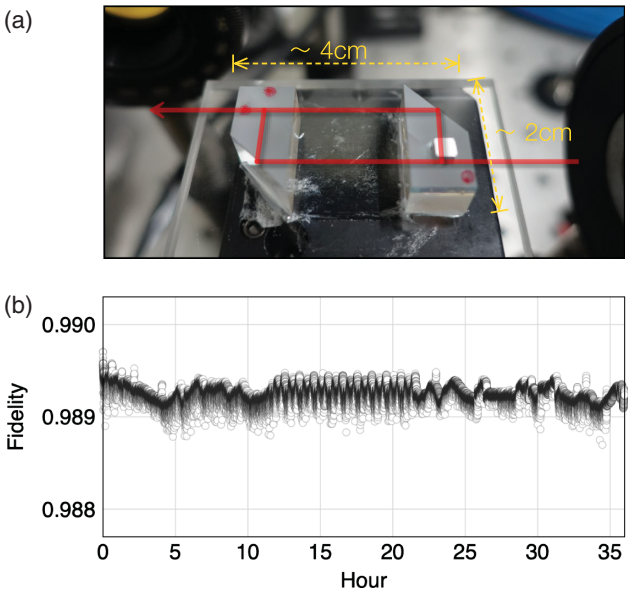

FIG. 2. The compact MZI and its stability. (a) Photograph of the compact MZI. (b) Long-term stability of the MZI. The MZI was tested with a local laser (FWHM ~ 1 nm) and multimode fiber to simulate the photon distorted by a turbulent free-space channel. The input beam is +45° polarized. The output of MZI is analyzed on $+45°/-45°$ polarization basis to calculate the fidelity. The MZI can maintain phase self-stabilization for more than one day. The average polarization fidelity is 0.989 (corresponding to an average contrast ratio of 92:1).

In our Letter, to simplify the device and realize long-term self-stability, we designed MZI into a compact one with a size of about 2×4 cm, as in Fig. 2(a). The MZI was constructed by precisely bonding two PBDs on a fused-silica substrate. The PBD was used to divide a beam into two parallel beams according to the polarization, and the translational distance between two beams was 10 mm. PBDs were positioned and adjusted with a hexapod and solidly bonded to the fused-silica substrate with ultraviolet adhesives of low strain. The path difference can be accurately controlled to less than 10 μm, which is within the coherence length of the entangled photon from the satellite. The use of full fused-silica material with a low coefficient of thermal expansion diminishes the temperature's impact. After the stress release, the MZI can preserve long-term self-stability for over 1 day [Fig. 2(b)] in the lab with a local laser. Then the MZI was mounted on the telescope and tested with the collected photons from a remote stellar (filtered into an FWHM of ~10 nm) to further verify outdoor robustness. A stable extinction ratio of more than 40:1 is observed for hours, corresponding to a fidelity of 0.976. The slightly lower fidelity here is mainly due to the imperfect MZI and the wide spectrum testing source. In addition to the above stationary target light source, the MZI was also tested with collected photons from the *Micius* satellite, emitted by a polarized cw laser (810 nm, FWHM ~ 0.6 nm). At the ground station (LJ), the output of the MZI is arranged for

measurement on $+45°/-45°$ basis with HWP and PBS. The polarized photon will pass through both paths of the MZI for interference. The measured average fidelity of the MZI in the satellite-to-ground channel is ~0.988.

At Bob's site (DLH), the telescope is polarization maintained. One motorized HWP rotates in real time to align the polarization direction according to the pointing to the satellite. Pockels cell and wave plate are ready for performing a unitary transformation to retrieve the quantum state into $|\chi\rangle_2 = \alpha|H\rangle_2 + \beta|V\rangle_2$ according to Alice's classical information of BSM result. However, the complete state-retrieve process requires the implementation of the active feed-forward technique [9,11,38]. Because of the lack of a practical quantum memory [39], the implementation of active feed-forward state retrieve is still a great challenge. A favorable solution is by performing tomography on the output and interpreting the results via postprocessing when the corrections are received. However, because of the low counting rate in our experiment, we employed a proof-of-principle method instead. Six quantum states to be transferred by Alice represent six poles of a universal alphabet on a Bloch sphere, which are linear polarization states $|H\rangle$, $|V\rangle$, $|+\rangle = (|H\rangle + |V\rangle)/\sqrt{2}$, $|-\rangle = (|H\rangle - |V\rangle)/\sqrt{2}$ and circular polarization states $|R\rangle = (|H\rangle + i|V\rangle)/\sqrt{2}$, $|L\rangle = (|H\rangle - i|V\rangle)/\sqrt{2}$. Bob's state analyzer comprising a PBS, an HWP, or a QWP is used to project the transferred state into either the ideal state or its orthogonal state, which can be predicted in advance corresponding to Alice's BSM outputs. By performing a two-photon coincidence measurement, we calculate the transferring fidelity as the ratio of the correct BSM coincidence events and the overall two-photon events. With this postprocessing method, Bob verifies photon 2's state. The standard interpretation of quantum mechanics told us whether the measurement is delayed or not does not affect the quantum part transferring [40]. The fidelity violation can be treated as a proof for demonstrating the feasibility of QST even without the state-retrieve process.

We prepare one polarization state in one orbit time. At both ground stations, the photons were collected into a multimode fiber with a core diameter of 320 μm and detected by the single-photon detector (SPD). All the time tags of photon-clicking events were recorded by a time-digital converter (TDC). The dark count of each detector was approximately 100 Hz. In addition, after filtering stray light, the background noise count is approximately 300 Hz for each detector. As illustrated in Fig. 1, the pulsed beacon laser from the satellite was divided on a beam splitter (BS). One part was guided to the camera working in the APT system, while the other part was attenuated and measured by a detector working as a time-synchronization signal also recorded in the TDC. The clock signal was also recorded to align the starting time between two ground stations. The data from two ground stations were postprocessed to record the twofold coincidence events. It should be noted that even the photon pair correlation was nonlocal; the data were interflowed through a classical channel, which excluded the superluminal communication in QST.

The fast-flying *Micius* lasted only for a duration of about 275 s in both DLH's and LJ's view between approximately 1:00 and 2:00 a.m. Beijing time each day. We obtained 924 two-photon coincidence events in total. The time window of the coincidence measurement is 4 ns. We calculated each fidelity of the six initial states and presented in Fig. 3. The fidelity of transferred states ranges from 0.76 to 0.86, with an average fidelity of 0.82 ± 0.01. This result is beyond the classical limit of fidelity of 2/3 for an arbitrary input qubit state or, equivalently, an alphabet of mutually unbiased states [38]. All presented data are raw without background subtraction.

The attenuation of the total two-downlink channel generally includes geometry attenuation due to the limited telescope aperture on the ground, atmospheric absorption, the efficiency of the optical system, the pointing error, and the detection efficiency. We measure it directly with the received count rates of single-photon detectors on the ground divided by the generation rate on the satellite. The total coverage range of the attenuation for these six orbits is about 64–82 dB.

In conclusion, we have proof-of-principle demonstrated 1200 km QST with the satellite-based prior entanglement distribution by following the Rome scheme. It provides a prototype for future complete satellite-based teleportation as an integral part of the large-scale quantum network. A highly stable interferometer applicable for atmosphere turbulence circumstance has been developed. We solve the problem of BSM interference with photons transmitting long distances in free-space channels, which is a bottleneck

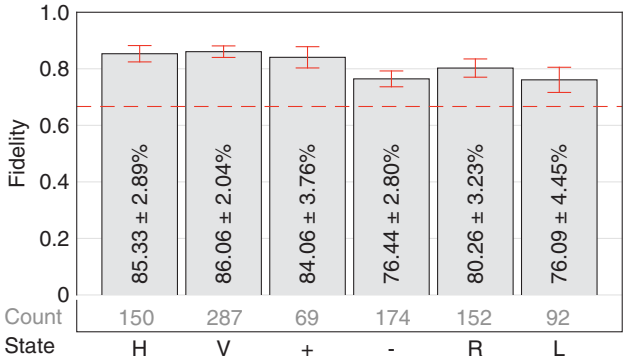

FIG. 3. Fidelity results of the six states. Data pertaining to the teleported states were collected in six orbits from 22 January, 2018 to 25 April, 2018. The data acquisition required favorable weather conditions when the *Micius* satellite flew in the common view of the LJ and DLH ground stations. As a result, the coincidence counts of the six states varied in each orbit. The two-photon coincidence events were acquired through an off-line data process. The observed fidelity of all six initial states have significantly exceeded the classical limit of 2/3 (dashed line). The error bars were calculated from Poissonian counting statistics.

in the previous long-distance quantum communication experiments. Even though we cannot accomplish full QST mainly due to lacking available practical quantum memory, our structure can still be beneficial for application in other quantum information scenarios. For instance, our setup can be upgradeable as integral in one-way blind quantum computation [41,42], which can be assisted by the teleportation technique without needing feed-forward or quantum memory. Our setup can also be applicable for some POVM (positive operator-valued measure)-based protocols [43,44].

We thank colleagues at the Shanghai Institute of Technical Physics, Institute of Optics and Electronics, National Space Science Center, China Xi'an Satellite Control Center, Yunnan Astronomical Observatory, Gaomeigu Station, Purple Mountain Observatory, and Qinghai Station for their management and coordination. We thank G.-B. Li, Z. Wang, W.-Y. Wang, W.-W. Ye, Y. Jiang, H.-B. Li, S.-J. Xu, Y.-Y. Yin, and X. Li for their long-term assistance in observation. We thank P. Xu for the discussion on data analysis. This work was supported by the National Key R&D Program of China (Grants No. 2017YFA0303900 and No. 2018YFE0200600), the Shanghai Municipal Science and Technology Major Project (Grant No. 2019SHZDZX01), the Anhui Initiative in Quantum Information Technologies, Science and Technological Fund of Anhui Province for Outstanding Youth (Grant No. 1808085J18), and the National Natural Science Foundation of China (Grants No. U1738201, No. 61625503, No. 11822409, No. 11674309, No. 11654005, and No. 61771443). Y. Cao was supported by the Youth Innovation Promotion Association of CAS (under Grant No. 2018492).

[*]These authors contributed equally to this work.

[1] C. H. Bennett, G. Brassard, C. Crépeau, R. Jozsa, A. Peres, and W. K. Wootters, Teleporting an Unknown Quantum State via Dual Classical and Einstein-Podolsky-Rosen Channels, Phys. Rev. Lett. **70**, 1895 (1993).

[2] C. H. Bennett and D. P. DiVincenzo, Quantum information and computation, Nature (London) **404**, 247 (2000).

[3] H. J. Briegel, W. Dür, J. I. Cirac, and P. Zoller, Quantum Repeaters: The Role of Imperfect Local Operations in Quantum Communication, Phys. Rev. Lett. **81**, 5932 (1998).

[4] H. J. Kimble, The quantum internet, Nature (London) **453**, 1023 (2008).

[5] D. Gottesman and I. L. Chuang, Demonstrating the viability of universal quantum computation using teleportation and single-qubit operations, Nature (London) **402**, 390 (1999).

[6] R. Raussendorf and H. J. Briegel, A One-Way Quantum Computer, Phys. Rev. Lett. **86**, 5188 (2001).

[7] D. Bouwmeester, J.-W. Pan, K. Mattle, M. Eibl, H. Weinfurter, and A. Zeilinger, Experimental quantum teleportation, Nature (London) **390**, 575 (1997).

[8] D. Boschi, S. Branca, F. De Martini, L. Hardy, and S. Popescu, Experimental Realization of Teleporting an Unknown Pure Quantum State via Dual Classical and Einstein-Podolsky-Rosen Channels, Phys. Rev. Lett. **80**, 1121 (1998).

[9] X.-M. Jin, J.-G. Ren, B. Yang, Z.-H. Yi, F. Zhou, X.-F. Xu, S.-K. Wang, D. Yang, Y.-F. Hu, S. Jiang, T. Yang, H. Yin, K. Chen, C.-Z. Peng, and J.-W. Pan, Experimental free-space quantum teleportation, Nat. Photonics **4**, 376 (2010).

[10] J. Yin *et al.*, Quantum teleportation and entanglement distribution over 100-kilometre free-space channels, Nature (London) **488**, 185 (2012).

[11] X.-S. Ma, T. Herbst, T. Scheidl, D. Wang, S. Kropatschek, W. Naylor, B. Wittmann, A. Mech, J. Kofler, E. Anisimova, V. Makarov, T. Jennewein, R. Ursin, and A. Zeilinger, Quantum teleportation over 143 kilometres using active feed-forward, Nature (London) **489**, 269 (2012).

[12] J.-G. Ren *et al.*, Ground-to-satellite quantum teleportation, Nature (London) **549**, 70 (2017).

[13] M. A. Nielsen, E. Knill, and R. Laflamme, Complete quantum teleportation using nuclear magnetic resonance, Nature (London) **396**, 52 (1998).

[14] H. Yonezawa, S. L. Braunstein, and A. Furusawa, Experimental Demonstration of Quantum Teleportation of Broadband Squeezing, Phys. Rev. Lett. **99**, 110503 (2007).

[15] S. Takeda, T. Mizuta, M. Fuwa, P. van Loock, and A. Furusawa, Deterministic quantum teleportation of photonic quantum bits by a hybrid technique, Nature (London) **500**, 315 (2013).

[16] J. F. Sherson, H. Krauter, R. K. Olsson, B. Julsgaard, K. Hammerer, I. Cirac, and E. S. Polzik, Quantum teleportation between light and matter, Nature (London) **443**, 557 (2006).

[17] M. D. Barrett, J. Chiaverini, T. Schaetz, J. Britton, W. M. Itano, J. D. Jost, E. Knill, C. Langer, D. Leibfried, R. Ozeri, and D. J. Wineland, Deterministic quantum teleportation of atomic qubits, Nature (London) **429**, 737 (2004).

[18] M. Riebe, H. Häffner, C. F. Roos, W. Hänsel, J. Benhelm, G. P. T. Lancaster, T. W. Körber, C. Becher, F. Schmidt-Kaler, D. F. V. James, and R. Blatt, Deterministic quantum teleportation with atoms, Nature (London) **429**, 734 (2004).

[19] L. Steffen, Y. Salathe, M. Oppliger, P. Kurpiers, M. Baur, C. Lang, C. Eichler, G. Puebla-Hellmann, A. Fedorov, and A. Wallraff, Deterministic quantum teleportation with feed-forward in a solid state system, Nature (London) **500**, 319 (2013).

[20] W. Pfaff, B. J. Hensen, H. Bernien, S. B. van Dam, M. S. Blok, T. H. Taminiau, M. J. Tiggelman, R. N. Schouten, M. Markham, D. J. Twitchen, and R. Hanson, Unconditional quantum teleportation between distant solid-state quantum bits, Science **345**, 532 (2014).

[21] F. De Martini, Teleportation: Who was first?, Phys. World **11**, 23 (1998).

[22] I. Marcikic, H. de Riedmatten, W. Tittel, H. Zbinden, and N. Gisin, Long-distance teleportation of qubits at telecommunication wavelengths, Nature (London) **421**, 509 (2003).

[23] Q.-C. Sun, Y.-L. Mao, S.-J. Chen, W. Zhang, Y.-F. Jiang, Y.-B. Zhang, W.-J. Zhang, S. Miki, T. Yamashita, H. Terai, X. Jiang, T.-Y. Chen, L.-X. You, X.-F. Chen, Z. Wang, J.-Y. Fan, Q. Zhang, and J.-W. Pan, Quantum teleportation with independent sources and prior entanglement distribution over a network, Nat. Photonics **10**, 671 (2016).

[24] R. Valivarthi, M. l. G. Puigibert, Q. Zhou, G. H. Aguilar, V. B. Verma, F. Marsili, M. D. Shaw, S. W. Nam, D. Oblak, and W. Tittel, Quantum teleportation across a metropolitan fibre network, Nat. Photonics **10**, 676 (2016).
[25] R. Ursin, T. Jennewein, M. Aspelmeyer, R. Kaltenbaek, M. Lindenthal, P. Walther, and A. Zeilinger, Communications—Quantum teleportation across the Danube, Nature (London) **430**, 849 (2004).
[26] H. de Riedmatten, I. Marcikic, W. Tittel, H. Zbinden, D. Collins, and N. Gisin, Long Distance Quantum Teleportation in a Quantum Relay Configuration, Phys. Rev. Lett. **92**, 047904 (2004).
[27] C.-Z. Peng, T. Yang, X.-H. Bao, J. Zhang, X.-M. Jin, F.-Y. Feng, B. Yang, J. Yang, J. Yin, Q. Zhang, N. Li, B.-L. Tian, and J.-W. Pan, Experimental Free-Space Distribution of Entangled Photon Pairs Over 13 km: Towards Satellite-Based Global Quantum Communication, Phys. Rev. Lett. **94**, 150501 (2005).
[28] S.-K. Liao *et al.*, Satellite-Relayed Intercontinental Quantum Network, Phys. Rev. Lett. **120**, 030501 (2018).
[29] J. Yin *et al.*, Satellite-to-Ground Entanglement-Based Quantum Key Distribution, Phys. Rev. Lett. **119**, 200501 (2017).
[30] J. Yin *et al.*, Satellite-based entanglement distribution over 1200 kilometers, Science **356**, 1140 (2017).
[31] S.-K. Liao *et al.*, Satellite-to-ground quantum key distribution, Nature (London) **549**, 43 (2017).
[32] P. Xu *et al.*, Satellite testing of a gravitationally induced quantum decoherence model, Science **366**, 132 (2019).
[33] H. Dai, Q. Shen, C. Z. Wang, S. L. Li, W. Y. Liu, W. Q. Cai, S. K. Liao, J. G. Ren, J. Yin, Y. A. Chen, Q. Zhang, F. Xu, C. Z. Peng, and J. W. Pan, Towards satellite-based quantum-secure time transfer, Nat. Phys. **16**, 848 (2020).
[34] J. Yin *et al.*, Entanglement-based secure quantum cryptography over 1,120 kilometres, Nature (London) **582**, 501 (2020).
[35] Y.-A. Chen *et al.*, An integrated space-to-ground quantum communication network over 4,600 kilometres, Nature (London) **589**, 214 (2021).
[36] G. Vallone, D. Dequal, M. Tomasin, F. Vedovato, M. Schiavon, V. Luceri, G. Bianco, and P. Villoresi, Interference at the Single Photon Level Along Satellite-Ground Channels, Phys. Rev. Lett. **116**, 253601 (2016).
[37] F. Vedovato, C. Agnesi, M. Schiavon, D. Dequal, L. Calderaro, M. Tomasin, D. G. Marangon, A. Stanco, V. Luceri, G. Bianco, G. Vallone, and P. Villoresi, Extending Wheeler's delayed-choice experiment to space, Sci. Adv. **3**, e1701180 (2017).
[38] S. Pirandola, J. Eisert, C. Weedbrook, A. Furusawa, and S. L. Braunstein, Advances in quantum teleportation, Nat. Photonics **9**, 641 (2015).
[39] S.-J. Yang, X.-J. Wang, X.-H. Bao, and J.-W. Pan, An efficient quantum lightmatter interface with sub-second lifetime, Nat. Photonics **10**, 381 (2016).
[40] X. S. Ma, J. Kofler, and A. Zeilinger, Delayed-choice gedanken experiments and their realizations, Rev. Mod. Phys. **88**, 015005 (2016).
[41] T. Morimae and K. Fujii, Blind quantum computation protocol in which Alice only makes measurements, Phys. Rev. A **87**, 050301(R) (2013).
[42] J. F. Fitzsimons, Private quantum computation: an introduction to blind quantum computing and related protocols, npj Quantum Inf. **3**, 23 (2017).
[43] S. Gómez, A. Mattar, E. S. Gómez, D. Cavalcanti, O. J. Farías, A. Acín, and G. Lima, Experimental nonlocality-based randomness generation with nonprojective measurements, Phys. Rev. A **97**, 040102(R) (2018).
[44] A. Tavakoli, M. Smania, T. Vértesi, N. Brunner, and M. Bourennane, Self-testing nonprojective quantum measurements in prepare-and-measure experiments, Sci. Adv. **6**, eaaw6664 (2020).